Available online at www.sciencedirect.com
SCIENCE DIRECT®
Polymer 45 (2004) 1033–1043
polymer
www.elsevier.com/locate/polymer

Novel application of reactive blending: tailoring morphology of PBT/SAN blends

Hideko T. Oyama[a,*], Tomoki Kitagawa[b], Toshiaki Ougizawa[b], Takashi Inoue[c], Martin Weber[d]

[a]*Research Center of Macromolecular Technology, National Institute of Advanced Industrial Science and Technology, Aomi, Kohtoh-ku, Tokyo 135-0064, Japan*
[b]*Department of Organic and Polymeric Materials, Tokyo Institute of Technology, Ookayama, Meguro-ku, Tokyo 152-8552, Japan*
[c]*Department of Polymer Science and Engineering, Yamagata University, Yonezawa 992-8510, Japan*
[d]*BASF Aktiengesellschaft, Polymer Research, GKT/B-B1, Ludwigschafen D-67056, Germany*

Received 8 August 2003; accepted 14 November 2003

Abstract

Reactive blending has been usually utilized to stabilize morphology and to improve the properties of multi-component polymer blends by generating copolymers in situ at the interface. However, the present study on blends composed of poly(butylene terephthalate) (PBT) and functionalized styrene–acrylonitrile random copolymer (SAN) demonstrates another possibility for this method, i.e. tailoring morphology and thereby controlling the properties of polymer blends. By varying reaction conditions it was demonstrated that blends could be formed having the same ratio of [PBT]/[SAN] but which possessed completely different microstructural forms: a sea–island morphology with and without micelles, a corded dispersed phase morphology, and a highly oriented, layer-like morphology.

Keywords: Reactive blending; Morphology; Reaction conditions

1. Introduction

Blends composed of a polyester and a functionalized polymer have been extensively studied. Several types of functional groups have been introduced as the counterpart of the polyester functionality in order to induce reactions between the two component polymers. Groups such as oxazoline (OXA) [1–3], maleic anhydride (MAH) [4–16], isocyanate (NCO) [17,18], and glycidyl methacrylate (GMA) [19–24] have been used.

First, in the reactive blending involving OXA, there are reports on PBT blends with OXA-grafted polypropylene [1], OXA-grafted polystyrene [2], OXA-grafted polyolefins (various) and SEBS [3]. All of these studies report that the presence of OXA reduces the particle size of the dispersed phase and improves adhesion between the two phases. The reaction between oxazoline and the carboxylic acid end of the PBT is the major reaction.

Second, in the reactive blending involving MAH, there are contradictory results reported in the literature on the reactivity between MAH and the polyester end groups. One group reports that MAH reacts with the hydroxyl terminal group of the polyester to produce an ester linkage [4–13]. Another group shows results that the reaction is unlikely to take place and that only secondary physical interactions occur [14–16].

For example, Kang et al. [7] found that blends composed of PBT and ethylene–vinyl acetate copolymer (EVA) grafted with MAH resulted in finely dispersed domains, showing that the functionalized EVA was able to compatibilize the blends through reaction. Tanrattanakul et al. [8] demonstrated that introduction of the MAH group to SEBS yielded finer dispersions of the minor phase and improved tensile properties in PET/SEBS-*g*-MAH blends. Lepers et al. [12,13] studied the effects of the reaction on the coalescence and interfacial tension of PET/PP blends in the presence of SEBS-*g*-MAH and reported reduction of interfacial tension and prevention of coalescence of the dispersed phase.

On the other hand, Shieh et al. [15] reported PP/PBT/PP-*g*-MAH blends, where PBT and PP-*g*-MAH hardly reacted. Therefore, they attempted to improve the reaction between

* Corresponding author. Tel.: +81-3-3599-8337; fax: +81-3-3599-8166.
E-mail address: hideko-oyama@aist.go.jp (H.T. Oyama).

0032-3861/$ - see front matter © 2003 Elsevier Ltd. All rights reserved.
doi:10.1016/j.polymer.2003.11.040

the component polymers by adding a third component, as will be mentioned in detail later.

Third, in the study on the reactive blending involving NCO, there are reports on PET/polypropylene (PP) grafted with 2-hydroxyethyl methacrylate–isophorone diisocyanate (PP-*g*-HI)[17] and PBT/ethylene–propylene elastomer functionalized with isocyanate groups [18]. The first paper reports that not only mechanical properties were improved by the interfacial reaction between the two component polymers but also that water absorption of the PET/PP-*g*-HI was much lower than that of PET/PP. This was because the hydrophobic PP particles had smaller particle size in the reactive system and consequently their larger surface area suppressed water absorption more efficiently.

Fourth, in the reactive blending involving glycidyl methacrylate (GMA) or epoxide groups, there are reports on PBT/epoxidized ethylene–propylene–diene rubber (eEPDM),[19] PBT/ethylene–methacrylate–glycidyl methacrylate terpolymer (E–MA–GMA),[20] and PBT/ABS/methyl methacrylate–glycidyl methacrylate–ethyl acrylate terpolymers (MGE) [21–23]. In the last system, the addition of MGE successfully reduced the scale of dispersion, provided morphology stability, and improved low temperature impact toughness of PBT/ABS blends. The authors report that some chemical residues (probably acids) in the emulsion-made ABS materials catalyze reactions of the GMA group and promote ring opening polymerization of the epoxide units, although other reaction pathways cannot be ruled out [23].

In the study of PBT blends either with ethylene–ethylacrylate–glycidyl methacrylate (E–EA–GMA) or with ethylene–ethylacrylate–maleic anhydride (E–EA–MAH) [24], it is reported that GMA has higher reactivity compared to MAH. Kalfoglou et al. [10] report on the reactivity of PET with different functional groups of compatibilizers in PET/HDPE blends: an ethylene–glycidyl methacrylate copolymer (E–GMA), an ethylene ethylacrylate–glycidyl methacrylate copolymer (E–EA–GMA), a hydrogenated styrene–butadiene–styrene copolymer grafted with maleic anhydride group (SEBS-*g*-MAH), and a MAH-modified ethylene–methyl acrylate copolymer (E–MeA-*g*-MAH). It is concluded that the compatibilizing effectiveness decreases in the order: E–GMA > E–EA–GMA > SEBS-*g*-MAH > E–MeA-*g*-MAH. Furthermore, van Aert et al. studied blends formed between PBT and poly(2,6-dimethyl-1,4-phenylene ether), PPE, functionalized with different reactive groups [25]. They concluded that the effectiveness of functional groups attached to the PPE chain decreases in the following order: carboxylic acid > amino > hydroxyl alkyl ≅ *t*-BOC-protected amino > methyl ester.

In the present study, PBT/SAN blends were prepared at different reaction conditions, e.g. by introducing different reactive groups to SAN and by adding catalyst or a coupling agent. This work will demonstrate new applications of reactive processing, in which a wide variety of blend morphologies can be obtained even at the same blend composition. It is expected that the different blend morphologies will result in different physical properties so that depending on the intended application a desirable blend morphology can be chosen by controlling the conditions of reactive processing.

2. Experimental

2.1. Materials

Table 1 lists characteristics of PBT and SAN samples used in this study and Fig. 1 shows their chemical structures. Two different types of reactive SANs, maleic anhydride-grafted SAN (SAN-MAH) and glycidyl methacrylate-grafted SAN (SAN-GMA), were prepared by radical polymerization in a pilot plant equipment consisting of a 10 l vessel and a degassing extruder. The weight ratio of [styrene]/[acrylonitrile]/[a repeating unit with the functional group] in the final product was 75/23/2 in both reactive SANs. The functionality of the reactive SANs was determined by infrared spectroscopy (IR) and the OH and COOH contents of PBT were estimated by potentiometric titration. For the determination of the COOH content, the material was first dissolved in a 1/1 mixture of phenol and *o*-dichlorobenzene (OCDB) at ca. 100 °C. Then, it was titrated by the tetra-butylammonium hydroxide solution. For the determination of the OH content, PBT was first dissolved in a mixture of pyridine, toluene and acetic anhydride. After keeping it for 1 h at 95 °C, the mixture was cooled down to room temperature and titrated with the KOH solution. As a control sample, SAN25 (AN content = 25 wt%) without any functional groups was used.

Ethyltriphenyl phosphonium bromide (ETPB) purchased from Aldrich and poly[methylene (phenylene isocyanate)]

Table 1
Sample characteristics

	M_n (g/mol)	M_w (g/mol)	T_g (°C)	T_m (°C)	Functionality (μmol/g)	η^* at 5 s^{-1} (Pa s)[a]
PBT	10,200	45,800	43	223	[COOH] 13 [OH] 101	2.2×10^3
SAN25	68,000	180,000	108	–	0	1.1×10^3
SAN-MAH	75,600	164,100	112	–	204	1.4×10^3
SAN-GMA	74,000	166,600	105	–	141	2.2×10^3

[a] Complex melt viscosity, η^*, measured at 250 °C.

(a) PBT

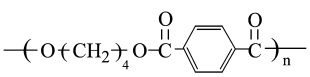

(b) SAN25 (x/y = 75/25 by weight)

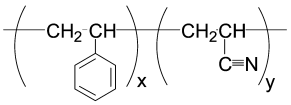

(c) SAN-MAH (x/y/z = 75/23/2 by weight)

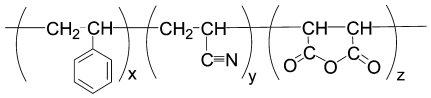

(d) SAN-GMA (x/y/z = 75/23/2 by weight)

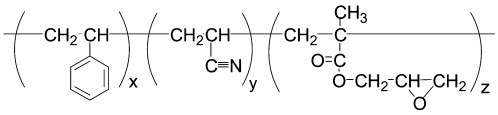

(e) ETPB

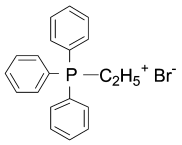

(f) PMPI

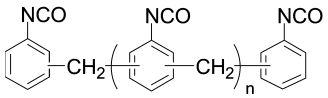

Fig. 1. Chemical structures of materials used in this study.

(PMPI) with 2.7 isocyanate groups per chain and a number average molecular weight of 360 supplied by BASF were used as received. These were employed respectively in some reactions as a catalyst and a coupler. Their structures are also shown in Fig. 1.

2.2. Melt viscosity

The complex dynamic viscosity, η^*, was measured at 250 °C with a rheometric dynamic spectrometer (Model RDS-7700) in a parallel-plate mode (plate radius 12.5 mm, gap 1.0 mm) with a 10% strain amplitude in the range between 0.1 and 500 s^{-1}.

2.3. Melt mixing

Materials were dried under vacuum (10^{-4} Torr) at 80 °C for 48 h in order to remove water prior to experiments. Melt mixing was carried out in a one gram-scale mixer (Mini Max Molder, CS-183 MM, Custom Scientific Instruments Inc.) at 250 °C under an average shear rate of 5 s^{-1}. The weight ratio of [PBT]/[SAN] was fixed at 70/30 except for special cases. During the mixing, a small amount of mixed melt (40 mg) was picked up by pincette at appropriate intervals and was quickly quenched in ice water to freeze the two phase structure in the residence times in the mixer.

2.4. Morphology analysis

The specimens were pre-stained using the vapor of ruthenium tetraoxide (RuO_4) and were microtomed at room temperature and then were re-stained prior to measurements by transmission electron microscopy (TEM, JEOL JEM-100CX). The RuO_4 preferentially stains the PBT phase over the SAN phase to provide a nice contrast in the TEM micrographs. It was confirmed that the observed morphology was representative by repeating the same experiments.

Furthermore, time-resolved light scattering measurements were carried out in order to measure the mean particle size of the dispersed phase. The quenched specimen was placed between a pair of cover glasses and melt-pressed to a thin film (ca. 40 μm thick) at 250 °C on a hot stage set in a light scattering apparatus. Then, the scattering profile was monitored, in which a polarized He–Ne gas laser of 632.8 nm wavelength was applied vertically to the film specimen on a hot stage kept at 250 °C. The goniometer trace of the scattered light from the sample was obtained under the V_v (parallel polarized) optical alignment. Details about the light scattering device have been described elsewhere [26].

2.5. Thermal analysis

A differential scanning calorimeter (Seiko SII DSC 6200) was operated with a heating rate of 10 °C min^{-1} under a N_2 atmosphere. The glass transition temperature, T_g, and the melting temperature, T_m, were obtained from the measurements.

3. Results and discussion

3.1. Comparisons between a non-reactive blend (PBT/SAN25) and reactive blends (PBT/SAN-MAH and PBT/SAN-GMA)

Light scattering measurements show a change in the mean particle size (D_{scatt}) of the SAN dispersed phase during melt mixing (Fig. 2). The intensity of scattered light monotonically decreased with an increase in the scattering angle, in which the mean diameter of the dispersed particles was estimated from the Debye–Bueche plot.

TEM shows the morphology of various PBT/SAN blends mixed at 250 °C for 9 min in the Mini Max Molder (Fig. 3). The darker region corresponds to the PBT phase stained by RuO_4, whereas the lighter region corresponds to the SAN phase. The reactive PBT/SAN-GMA (Figs. 2(c) and 3(c)) yielded finer particles than the non-reactive PBT/SAN25 (Figs. 2(a) and 3(a)). By contrast, the mean particle size of

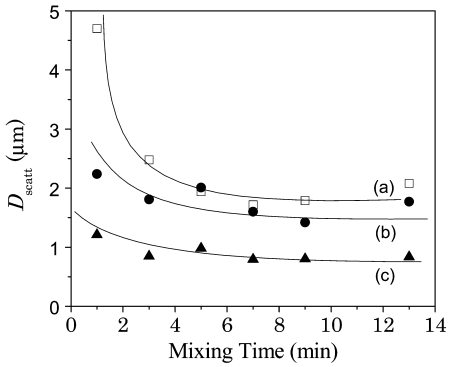

Fig. 2. Change in the mean particle size, D_{scatt}, of the SAN dispersed phase during melt mixing at 250 °C. [(a) (70/30) PBT/SAN25, (b) (70/30) PBT/SAN-MAH, and (c) (70/30) PBT/SAN-GMA].

PBT/SAN-MAH blend was slightly smaller than that of the non-reactive blend. The morphology of the PBT/SAN-MAH (Fig. 3(b)) was very similar to that of the non-reactive blend (Fig. 3(a)).

Next, the static stability during isothermal annealing of these three blends was examined. Fig. 4 shows a change in the mean particle size of the SAN dispersed phase as a function of the annealing time at 250 °C. The mean particle

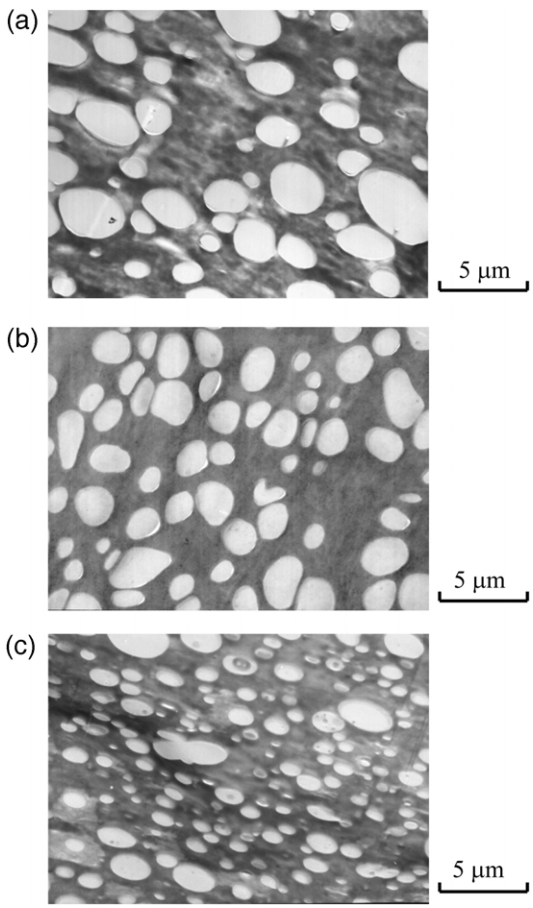

Fig. 3. TEM micrographs of the blends melt mixed at 250 °C for 9 min. [(a)–(c) are the same as those in Fig. 2].

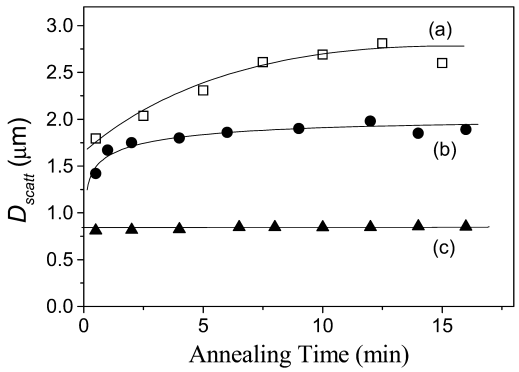

Fig. 4. Effects of isothermal annealing at 250 °C on the mean particle size, D_{scatt}, of the SAN dispersed phase. [(a)–(c) are the same as those in Fig. 2].

size of PBT/SAN25 (Fig. 4(a)) and PBT/SAN-MAH (Fig. 4(b)) increased with the annealing time, whereas that of PBT/SAN-GMA (Fig. 4(c)) remained constant. Thus, the results given in Figs. 2–4 consistently confirm that PBT/SAN-GMA produces a sufficient amount of copolymers at the interface during melt mixing, whereas PBT/SAN-MAH does not.

The evidences presented above indicate that copolymers formed by the reaction of the epoxide group in SAN-GMA with either COOH or OH groups located at the PBT chain ends proceed sufficiently to produce the emulsifying effects. Both end groups of PBT are considered to act as nucleophiles, reacting with the epoxides through nucleophilic substitution. The reaction of the epoxide group either with the COOH group or with the OH group would be addition esterification or etherification, respectively, both of which generate the secondary hydroxyl group [27]. In addition, it is also suggested that the two kinds of crosslinking reactions would proceed simultaneously [20]. One is through a reaction between the epoxide group and the secondary hydroxyl group pre-generated by a reaction occurred between PBT and SAN-GMA. The other is through a reaction of difunctional PBT chains, which will function as a crosslinking agent.

However, there is another report investigating the reactivity between the PBT end groups and the epoxide group in PBT/SAN/MGE (methyl methacrylate–glycidyl methacrylate–ethyl acrylate terpolymer), which presents a conflicting result. This study suggests that the reaction of the epoxide group with the COOH group occurs but the reaction with the OH group does not [28].

3.2. Effects of ETPB on morphology of PBT/SAN-GMA

The effects of acceleration of the reactions between PBT and SAN-GMA on blend morphology was investigated by using the catalyst ethyltriphenyl phosphonium bromide (ETPB). Ethyltriphenyl phosphonium salts have been used commercially as catalysts to produce solid epoxy resins [29,30] and epoxy ester resins [31]. Reactions of the epoxide group with –OH and –COOH groups are utilized in these

processes. Some papers have reported studies of polymer blends using the above reactions [32–37].

Chang's group studied PBT/ABS/SAG (styrene–acrylonitrile–glycidyl methacrylate) blends in the presence of ETPB, since rubber toughening of PBT/ABS was not satisfactory [32]. It was observed that the addition of ETPB increased the tensile elongation and the falling weight impact energy. It was also reported that addition of amounts as small as 50 ppm of ETPB catalyst was able to promote the grafting reaction to obtain good mechanical properties. However, it was found that amounts of 2000 ppm or higher might catalyze degradation of the blend at a significantly slower rate than the grafting reaction.

The reaction involving ETPB is considered to proceed as shown in Scheme 1. The ETPB catalyst would first dissociate and carry out a nucleophilic attack (Eq. (1)), which opens the epoxy ring located in SAN-GMA to form product ((A)) (Eq. (2)). Then, ((A)) can react either with –COOH (Eq. (3)) or with –OH (Eq. (4)) of the PBT end groups [33]. In this manner PBT-*co*-SAN would be generated efficiently at the interface.

The morphology of the blends prepared with various concentrations of ETPB is shown in Fig. 5, in which the catalyst was added prior to melt mixing. PBT/SAN-GMA (prepared without catalyst) yielded a spherical dispersed phase (Fig. 5(a)). However, as the ETPB concentration increased, a corded dispersed phase appeared. In the blend prepared with 1400 ppm of ETPB catalyst, the spherical dispersed phase hardly existed any more and the corded dispersed phase was mainly formed (Fig. 5(c)).

Next, the effect of time of the ETPB addition was investigated. Fig. 6(a) and (b) show the morphology of the blends, in which 900 ppm of ETPB was added prior to melt mixing and 5 min after the onset of melt mixing, respectively. With addition prior to melt mixing the corded dispersed phase was mainly formed (Fig. 6(a)), whereas with addition after the onset of melt mixing the spherical dispersed phase appeared (Fig. 6(b)). The result clearly indicates that the corded dispersed phase is generated only when ETPB contributes to the reaction in the early stages of melt mixing.

The group of Macosko [38–40] describes a mechanism of morphology development of polymer blends

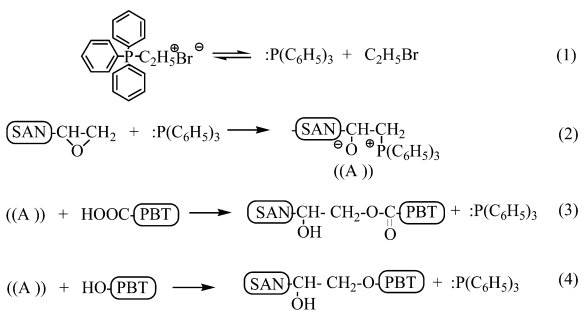

Scheme 1. Possible reactions between ETPB and the terminal groups of PBT.

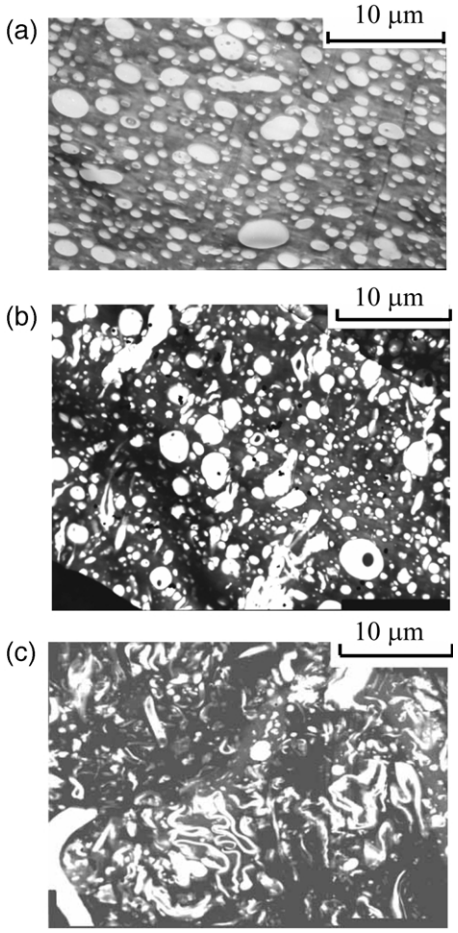

Fig. 5. TEM micrographs of (70/30/x) PBT/SAN-GMA/ETPB melt mixed at 250 °C (9 min). ETPB was added prior to melt mixing. ([ETPB] = (a) 0 ppm, (b) 100 ppm, and (c) 1400 ppm, respectively).

during melt mixing. As pellets of the minor component soften, shear caused by the major component first pulls sheets out of a large mass of the minor dispersed phase. Then, holes are developed in the sheets, which results in a fragile lace structure or strands. At the end, these are broken up by developing holes or tearing into droplets. In reactive blends during this process, copolymers at the interface reduce interfacial tension allowing sheets and strands to be drawn thinner and prevent drop coalescence. As a result this forms the finer droplets with submicron size.

In the absence of ETPB catalyst, PBT-*co*-SAN graft copolymers, which play the role of emulsifier to prevent particle coalescence and to reduce interfacial tension, are generated predominantly through a reaction between the epoxide group in SAN-GMA and the carboxylic acid end group of PBT. On the other hand, in the presence of ETPB catalyst, the overall reactions are accelerated as shown in Scheme 1 and the reaction with the hydroxyl end group of PBT in Eq. (4) becomes facilitated [37,41]. This would produce a crosslinked network of copolymers at the interface. The corded domains are probably formed because

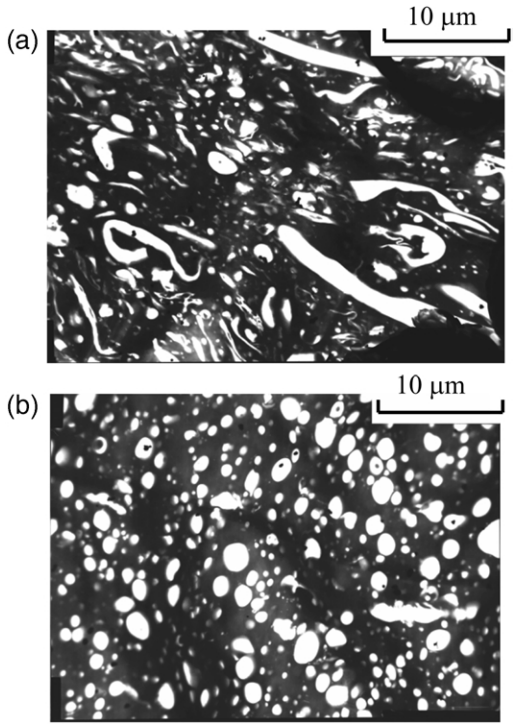

Fig. 6. Difference in time to add 900 ppm of ETPB. The blends were mixed at 250 °C totally for 9 min. [(a) ETPB was added prior to the onset of melt mixing, (b) ETPB was added 5 min after the onset of melt mixing].

the so-obtained crosslinkage prevents the stretched strands in Macosko's scheme formed in the initial stage from being broken into droplets. This might be the reason for the corded dispersed phase to remain even at 9 min of the melt mixing.

Next, the effect of the shear rate on blend morphology in the presence of ETPB was studied. Fig. 7 shows morphology of the blends at 9 min of melt mixing, which were prepared at various shear rates using 900 ppm of ETPB catalyst in all cases. When the shear rate became smaller than 5 s^{-1}, a long corded dispersed phase appeared (Fig. 7(a)). In contrast, when the shear rate became larger than 5 s^{-1}, the corded dispersed phase hardly existed and only the spherical dispersed phase appeared (Fig. 7(c)). These results imply that at the lower shear rate the force was insufficient to break up the stretched strands into droplets and that the network of copolymers were formed more effectively at the interface. On the other hand, at the higher shear rate where new interface was constantly formed, the formation of the crosslinked copolymers at the interface was suppressed and thereby the break-up of the corded domain into droplets was promoted.

3.3. Effects of PMPI on the morphology of PBT/reactive SAN blends

Ju et al. [16] investigated PET/PS/SMA (styrene–maleic anhydride random copolymer with 8 wt% MA) blends and reported that the reaction between anhydride groups of SMA and hydroxyl groups of PET was unlikely to occur.

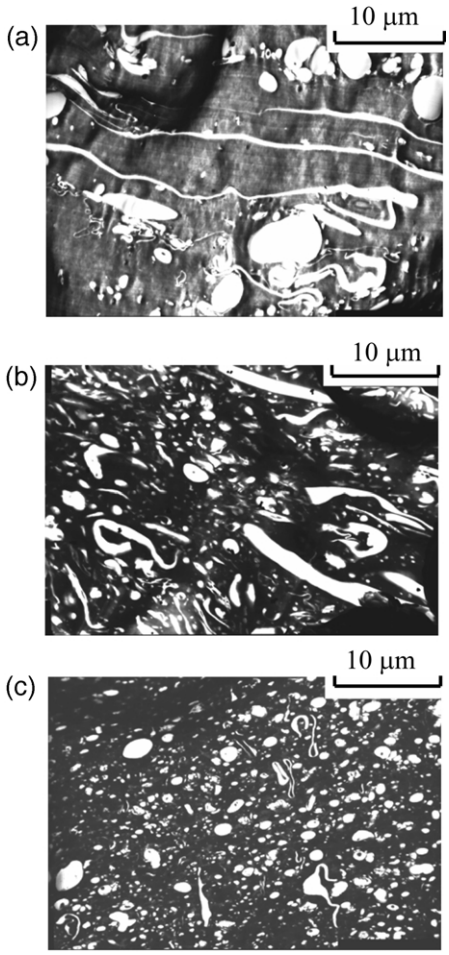

Fig. 7. TEM micrographs of (70/30/0.09) PBT/SAN-GMA/ETPB melt-mixed at 250 °C for 9 min under various shear rates. Average shear rate is (a) 2.5 s^{-1}, (b) 5 s^{-1}, and (c) 7.5 s^{-1}, respectively.

Then, they demonstrated that the reaction took place in the presence of PMPI, which assisted in the formation of desirable PET-*co*-PMPI-*co*-SMA. The resultant blends exhibited higher viscosity, finer phase domains, and improved mechanical properties. Therefore, in the present study PMPI was introduced to PBT/SAN-MAH blends which did not have enough reaction between the component polymers, and the effect of PMPI on morphology was studied in detail. First, the reactivity between PMPI and each component polymer was investigated by measuring the melt viscosity of their mixture. Second, mechanisms of morphology development in different types of PBT/reactive SAN/PMPI blends were investigated.

3.3.1. Reactivity of PMPI with each component polymer

Scheme 2 summarizes the possible reactions of PMPI in the present systems [42]. The isocyanate group of PMPI reacts with the terminal groups of PBT, i.e. both -COOH and -OH, where urethane formation (Eq. (5)) would be more dominant than amide formation (Eq. (6)). In SAN-MAH, the carboxylic acid groups are first generated as a result of ring

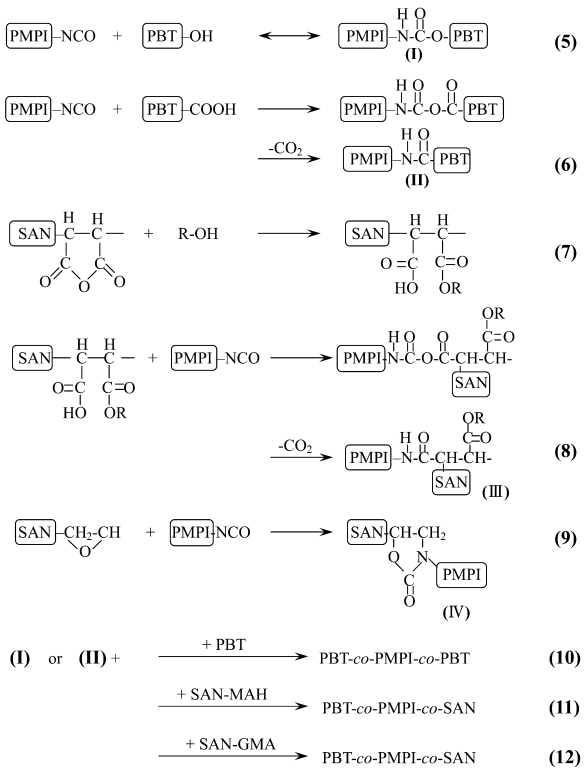

Scheme 2. Possible reactions of PMPI with component polymers.

opening of MAH, which is induced by a hydroxyl-containing compound (Eq. (7)). Then, the resultant COOH group would react with PMPI in the same way as Eq. (6) (Eq. (8)). In SAN-GMA, the reaction with PMPI would form the oxazoline group (IV) (Eq. (9)), although this is expected to be a minor reaction.

The PMPI molecule with 2.7 NCO groups per chain would function not only as a chain extender of PBT (Eqs. (5) and (6)) but also as a joint to create PBT-*co*-PMPI-*co*-PBT (Eq. (10)) and PBT-*co*-PMPI-*co*-SAN (Eqs. (11) and (12)). Here, the products shown in Eqs. (10)–(12) denote the kinds of components participating in the copolymer formation, not the architecture of the copolymer. Similarly the products (III) and (IV), if formed, can react with PBT through the multifunctional PMPI, resulting in the PBT-*co*-PMPI-*co*-SAN copolymers.

Next, the reactivity between PMPI and a component polymer was actually investigated by rheometric dynamic spectrometer measurements. Specimens containing PMPI were prepared by mixing the polymer and PMPI at 250 °C for 9 min in the Mini Max Molder. Fig. 8 shows the complex melt viscosity, η^*, as a function of the shear rate at 250 °C under 10% strain amplitude. Fig. 8(a) shows that the η^* of PBT was remarkably elevated by the addition of PMPI. This clearly indicates that an increase in molecular weight of PBT occurred as a result of the reaction between PBT and PMPI, presumably through the reactions shown by Eqs. (5) and (10). When additional PMPI was added to PBT, the reaction was enhanced. Fig. 8(b) shows that the η^* of SAN-GMA was similarly raised by the addition of PMPI but to a smaller extent. This gives evidences for reaction between SAN-GMA and PMPI, as also shown by Eq. (9).

By contrast, the melt viscosity of SAN-MAH and SAN25 shown in Fig. 8(c) and (d), respectively, did not increase by

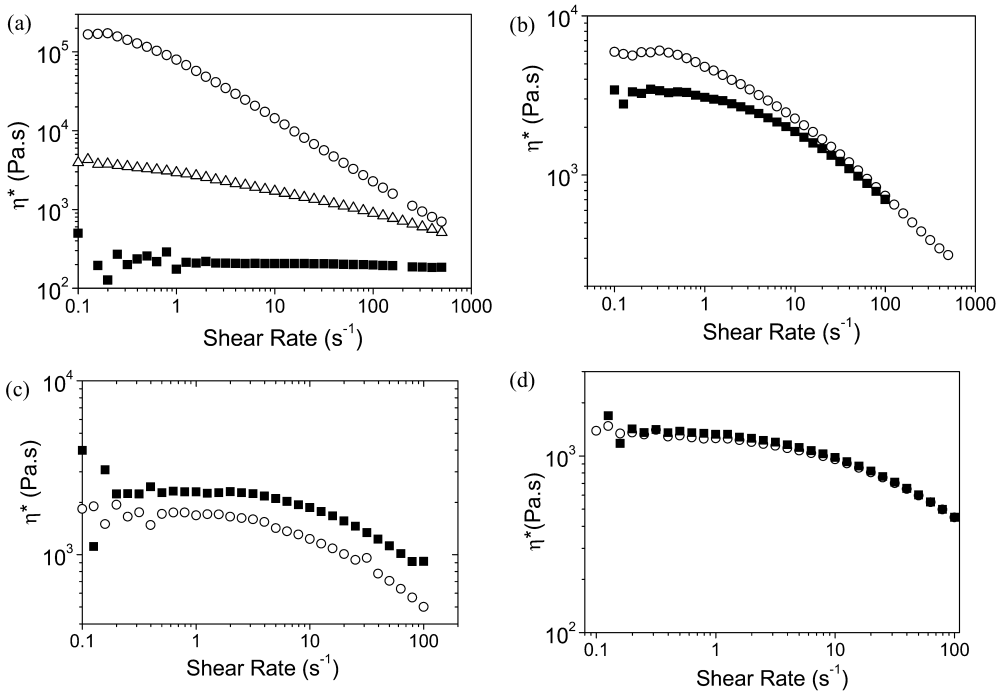

Fig. 8. Complex melt viscosity, η^*, of each component polymer in the presence of PMPI. [(a) ■ neat PBT, ○ (1.3 g PBT + 50 mg PMPI mixed at 250 °C for 9 min), △ (1 g PBT + 8 mg PMPI mixed at 250 °C for 9 min), (b) ■ neat SAN-GMA, ○ (1 g SAN-GMA + 50 mg PMPI mixed at 250 °C for 9 min), (c) ■ neat SAN-MAH, ○ (1 g SAN-MAH + 50 mg PMPI mixed at 250 °C for 9 min), (d) ■ neat SAN25, ○ (1 g SAN25 + 50 mg PMPI mixed at 250 °C for 9 min)].

addition of PMPI. This implies that there would be no reactions occurring between SAN-MAH and PMPI and between SAN25 and PMPI, so the reaction shown by Eq. (8) is negligible.

Therefore, taking into a consideration that there was little reaction between SAN-MAH and PBT, the reaction shown by Eq. (11) should be considered to be insignificant. Instead, the reaction shown by Eq. (10) would be the most dominant followed by the reaction shown by Eq. (12). The former would yield PBT-*co*-PMPI-*co*-PBT with large molecular weight in the PBT phase and the latter would generate PBT-*co*-PMPI-*co*-SAN at the interface.

3.3.2. Morphology of PBT/SAN/PMPI blends

Although the morphology of PBT/SAN25, PBT/SAN-MAH, and PBT/SAN-GMA blends prepared in the absence of PMPI shown in Fig. 3(a)–(c), respectively, had an ordinary sea–island morphology consisting of a dispersed phase of the SAN minor component in a matrix of the PBT major component, the morphology of blends prepared in the presence of PMPI showed a completely different structure at the same ratio of the component polymers (Fig. 9). These blends were prepared by melt mixing at 250 °C for 9 min in a similar manner. In the case of (70/30/5) PBT/SAN25/PMPI and (70/30/5) PBT/SAN-MAH/PMPI, the blends formed highly oriented structures (Fig. 9(a) and (b)). On the other hand, (70/30/0.8) PBT/SAN-GMA/PMPI formed the sea–island morphology containing a large number of fine dispersed domains (Fig. 9(c)). (The melt viscosity became too high for the Mini-Max Molder to rotate the (70/30/5) PBT/SAN-GMA/PMPI.) The fine domains with diameter of about 50 nm probably correspond to micelles. Special attention has to be paid to the scale given in each figure. Thus, the blends formed show completely different morphology even with the same [PBT]/[SAN] ratio depending on the reaction conditions. The mechanism of the morphology development will be discussed in the next section.

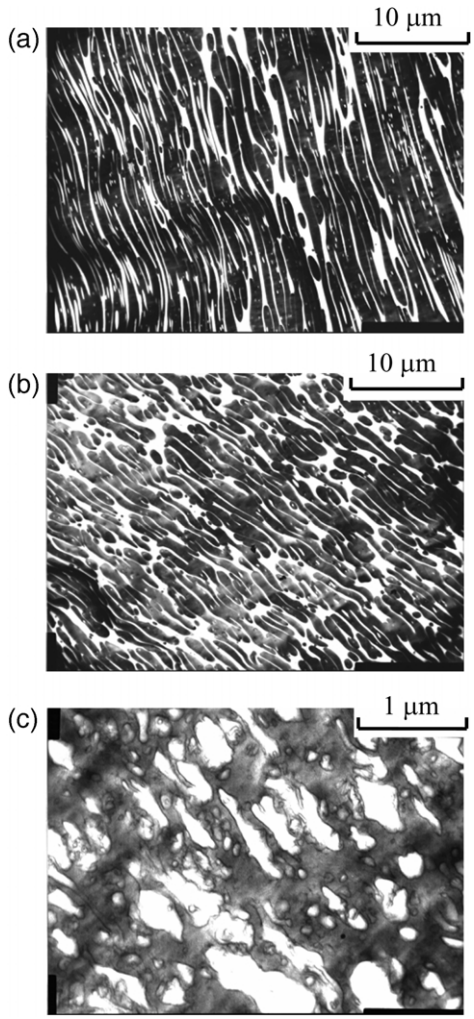

Fig. 9. TEM micrographs of blends mixed at 250 °C for 9 min in the presence of PMPI. [(a) (70/30/5) PBT/SAN25/PMPI, (b) (70/30/5) PBT/SAN-MAH/PMPI, and (c) (70/30/0.8) PBT/SAN-GMA/PMPI].

3.3.3. Mechanism of morphology development in the presence of PMPI

3.3.3.1. PBT/SAN25/PMPI and PBT/SAN-MAH/PMPI. It was mentioned previously that the maleic anhydride group incorporated into SAN hardly reacted either with –OH or with –COOH in PBT. Here for convenience, both PBT/SAN25/PMPI and PBT/SAN-MAH/PMPI will be treated as blends that do not have copolymers at the interface.

In non-reactive blends composed of dissimilar polymers, the major component usually tends to become the matrix, while the minor component tends to become the dispersed phase. In a symmetrical blend (50/50), the component with the lower viscosity tends to be the matrix and the one with the higher viscosity to be the dispersed phase. The following equation was proposed by Chen and Su [43] to predict the onset of phase inversion in a binary blend;

$$\frac{\phi_{hv}}{\phi_{lv}} = 1.2\left(\frac{\eta_{hv}}{\eta_{lv}}\right)^{0.3} \tag{13}$$

where the subscripts 'hv' and 'lv' denote the phase with the higher and the lower viscosity, respectively, and ϕ_{hv} and ϕ_{lv} are their respective volume fractions.

At the average shear rate in the present study, 5 s^{-1}, the complex melt viscosity, η^*, of the mixture of (PBT + PMPI), (SAN25 + PMPI), and (SAN-MAH + PMPI) was 2.4×10^4, 1.1×10^3, and 1.5×10^3 (Pa s), respectively. The weight ratio of [PBT]/[SAN]/[PMPI] for which phase inversion would be initiated in the present study was predicted to be 71/29/5 for PBT/SAN25/PMPI and 73/27/5 for PBT/SAN-MAH/PMPI, respectively, according to Eq. (13). If the amount of PBT is larger than the predicted value, the PBT phase would become the matrix. On the contrary, if the amount of PBT is smaller than the predicted value, phase

inversion would occur, and the PBT phase would become the dispersed phase.

Therefore, in order to examine the validity of Eq. (13), the effect of the blend composition on the morphology was investigated. Fig. 10(a)–(d) show the morphology of PBT/SAN25/PMPI at mixing weight ratios of 90/10/5, 80/20/5, 70/30/5, and 60/40/5, respectively. At the [PBT]/[SAN] weight ratio of 90/10 and 80/20 (Fig. 10(a) and (b)), the PBT major component was the matrix and the SAN minor component was the dispersed phase so that phase inversion did not occur. However, at the [PBT]/[SAN] weight ratio of 70/30 (Fig. 10(c)), a highly oriented co-continuous-like structure appeared. This ratio is almost the predicted ratio where the phase inversion would be initiated. The transition of the morphology was also observed even after 3 min of melt mixing, which indicated that the reaction between PBT and PMPI is very fast. Even after only 3 min of melt mixing, η^* of the PBT phase increased from 2×10^2 to over 1.38×10^4 (Pa s) according to estimates from Eq. (13). Furthermore, the phase inversion did occur at 60/40/5 PBT/SAN/PMPI (Fig. 10(d)). Thus, all experimental results followed the prediction of Eq. (13) as for the morphological transformation.

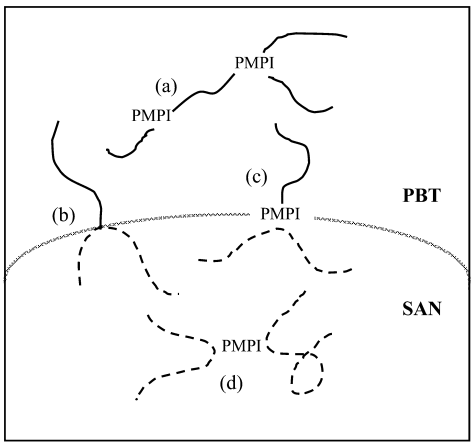

Fig. 11. Possible molecular architectures in PBT/SAN-GMA/PMPI blends. [(a) PBT-*co*-PMPI-*co*-PBT, (b) PBT-*co*-SAN, (c) PBT-*co*-PMPI-*co*-SAN, and (d) SAN-*co*-PMPI-*co*-SAN, respectively].

3.3.3.2. PBT/SAN-GMA/PMPI. One of the potential structures created in this system is illustrated in Fig. 11, although various reactions may be involved in this complex system. (1) In the PBT phase a reaction of PMPI with PBT would mainly cause chain extension or crosslinking of PBT in the

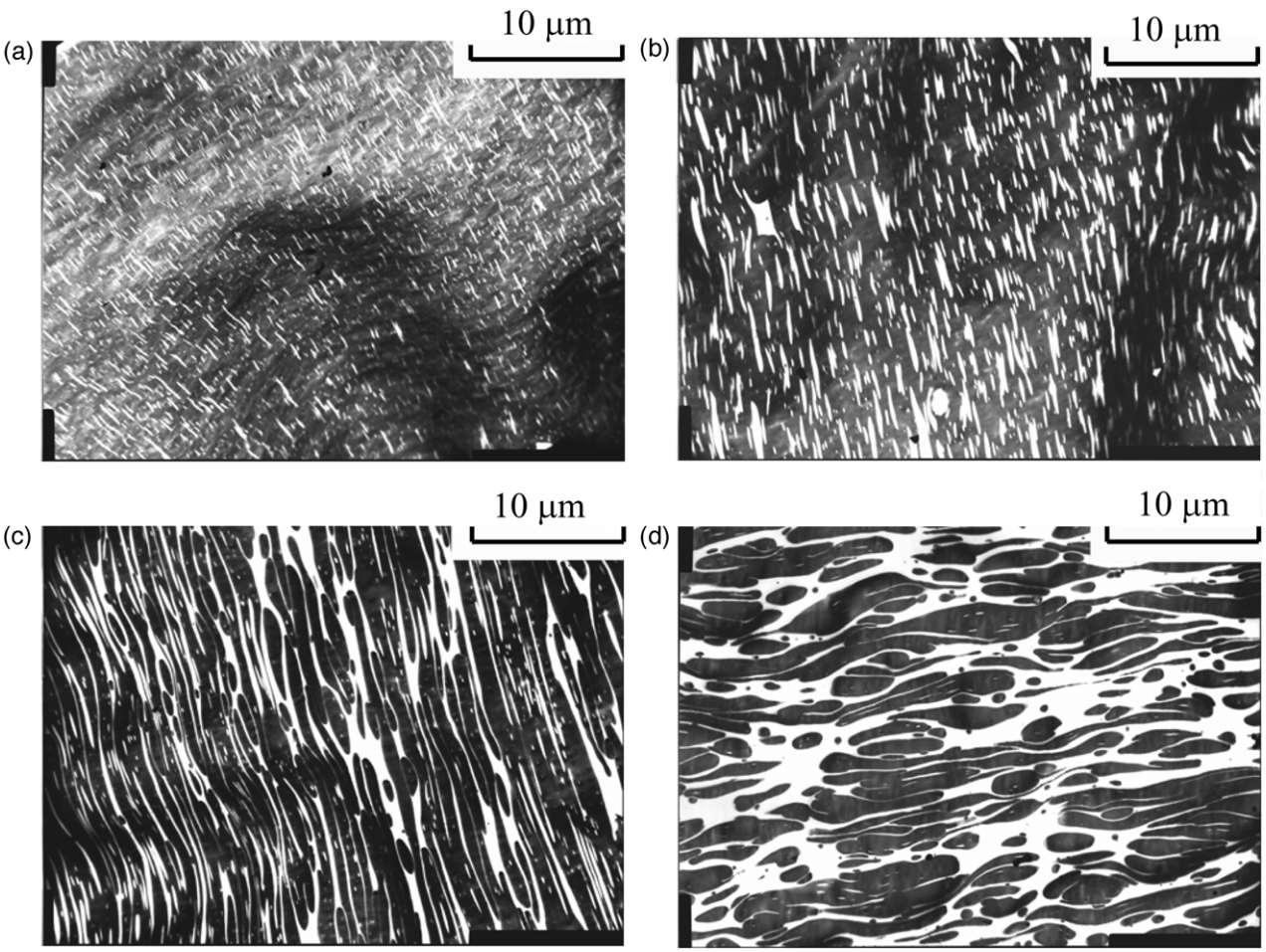

Fig. 10. Change in morphology of the PBT/SAN25/PMPI blends as a function of the blend composition. Blends were prepared by melt mixing at 250 °C for 9 min. ([PBT]/[SAN25]/[PMPI] weight ratio = (a) 90/10/5, (b) 80/20/5, (c) 70/30/5, and (d) 60/40/5, respectively).

PBT phase. (2) At the interface two kinds of copolymers would exist; PBT-*co*-SAN and PBT-*co*-PMPI-*co*-SAN. 3) In the SAN phase a reaction of PMPI with SAN-GMA would cause crosslinking.

Phase inversion was not observed in this system. Although the validity of Eq. (13) is questionable in this system because the equation was originally proposed to blends not containing copolymers, this might be because the increase of the complex melt viscosity in (1 g PBT + 8 mg of PMPI) was much lower than that in (1.3 g PBT + 50 mg of PMPI) (Fig. 8(a)) so that phase inversion did not occur as shown in Fig. 9(c).

Next, reasons will be presented to explain why the PBT/SAN-GMA/PMPI blend generated very fine particles. In reactive blends, it is reported that pull-out of copolymer chains from the interfacial region is induced by external shear forces [44–46]. Charoensirisomboon et al. [46] reported that a large number of copolymers are formed in situ even in the early stages of mixing and that they can escape or be pulled out by external shear forces from the interfacial region into the matrix as micelles. They report that block copolymers with a linear chain structure are more easily pulled out than graft copolymers with a branch structure, with graft copolymers having trunk chains located in the dispersed phase (inverse Y-shape) are hardly pulled out. Although the architecture of copolymers in this system is more complicated, small particles like micelles were clearly observed. The extension of the PBT chains brought about as a result of the reaction with PMPI might also facilitate the pull-out of copolymers and/or the break-up of the dispersed phase in the presence of copolymers at the interface.

The morphology at the early stage of melt mixing in the PBT/SAN-GMA/PMPI blend was investigated and its result is shown in Fig. 12. Very fine particles probably corresponding to micelles already existed even at 1 min after the onset of mixing, as shown in Fig. 12(a). The large domains stayed in the vicinity of the fine particles so that the micelles could be considered to be generated from the large domains. At 3 min after the onset of mixing, fine particles were dispersed uniformly in the matrix and the large domains completely disappeared (Fig. 12(b)).

In summary, it has been demonstrated in this report that blend morphology even at the same composition generated by reactive processing can be altered by changing the reaction conditions: the kind of reactive pairs, the shear rate, additives such as catalysts and couplers. These results clearly indicate that reactive processing can be utilized to tailor the blend morphology and properties for different applications, besides to stabilize the blend morphology thereby improving its mechanical properties.

4. Conclusions

PBT/SAN blends prepared without any additives have ordinary sea–island morphology. However, addition of ETPB to the mixture of PBT and SAN generated a blend morphology with a corded dispersed phase, which was probably because of in situ formed cross-linked copolymers at the interface. Furthermore, addition of PMPI induced the formation of a wide variety of morphology types even at the same composition including a highly oriented structure and a sea–island morphology with a large number of finely dispersed domains. It is confirmed that PMPI reacts with both PBT and SAN-GMA, but not with SAN-MAH. The reaction between PBT and PMPI was the most significant, and resulted in a large increase in the melt viscosity of the PBT phase.

In summary, the present study demonstrated that by controlling reaction conditions it is possible to form blends having the same ratio of the component polymers but possessing completely different morphology. Thus, the study shows the possibility of tailoring blend morphology for different applications.

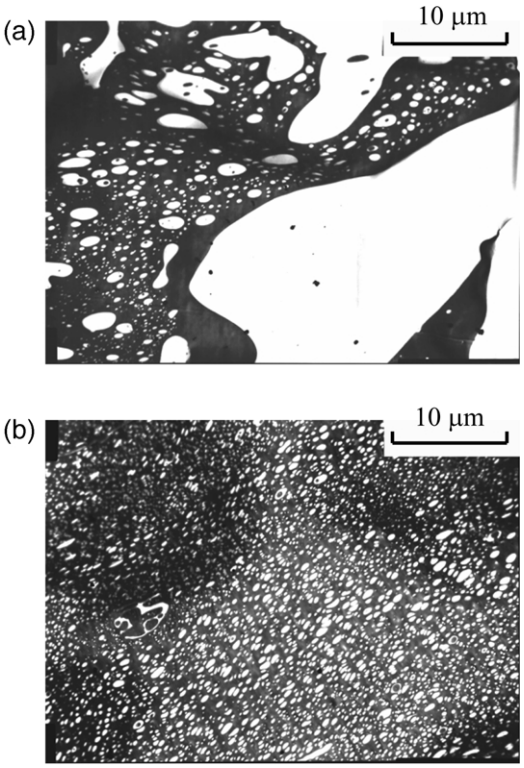

Fig. 12. TEM micrographs of the early stage of melt mixing in (70/30/0.8) PBT/SAN-GMA/PMPI blends. [(a) mixed for 1 min, (b) mixed for 3 min].

References

[1] Vainio T, Hu GH, Lambla M, Seppälä J. J Appl Polym Sci 1996;61:843–52.
[2] Lee S, Park OO. Polymer 2001;42:6661–8.
[3] Vocke C, Anttila U, Heino M, Hietaoja P, Seppälä J. J Appl Polym Sci 1998;70:1923–30.

[4] Immirzi B, Laurienzo P, Malinconico M, Martuscelli E. J Polym Sci, Part A: Polym Chem 1989;27:829–38.
[5] Yuan Y, Ruckenstein R. J Appl Polym Sci 1998;67:913–9.
[6] Hu GH, Sun YJ, Lambla M. Polym Engng Sci 1996;36:676–84.
[7] Kang TK, Kim Y, Kim G, Cho WJ, Ha CS. Polym Engng Sci 1997;37:603–14.
[8] Tanrattanakul V, Perkins WG, Massey FL, Moet A, Hiltner A, Baer E. J Mater Sci 1997;32:4749–58.
[9] Cecere A, Greco R, Ragosta G, Scarinzi G, Taglialatela A. Polymer 1990;31:1239–44.
[10] Kalfoglou NK, Skafidas DS, Kallitsis JK, Lambert JC. Polymer 1995;36:4453–62.
[11] Kalfoglou NK, Skafidas DS, Kallitsis JK. Polymer 1996;37:3387–95.
[12] Lepers JC, Favis BD, Tabar RJ. J Polym Sci, Part B: Polym Phys 1997;35:2271–80.
[13] Lepers JC, Favis BD, Lacroix C. J Polym Sci, Part B: Polym Phys 1999;37:939–51.
[14] Basu D, Banerjee A. J Appl Polym Sci 1997;64:1485–7.
[15] Shieh YT, Liao TN, Chang FC. J Appl Polym Sci 2001;79:2272–85.
[16] Ju MY, Chang FC. Polymer 2000;41:1719–30.
[17] Bae TY, Park KY, Kim DH, Suh KD. J Appl Polym Sci 2001;81:1056–62.
[18] Jun JB, Park JG, Kim DH, Suh KD. Eur Polym J 2001;37:597–602.
[19] Wang XH, Zhang HX, Wang ZG, Jiang BZ. Polymer 1997;38:1569–72.
[20] Martin P, Devaux J, Legras R, van Gurp M, van Duin M. Polymer 2001;42:2463–78.
[21] Hage E, Hale W, Keskkula H, Paul DR. Polymer 1997;38:3237–50.
[22] Hale W, Lee JH, Keskkula H, Paul DR. Polymer 1999;40:3621–9.
[23] Hale W, Keskkula H, Paul DR. Polymer 1999;40:3665–76.
[24] Hert M. Angew Makromol Chem 1992;196:89–99.
[25] van Aert HAM, van Steenpaal GJM, Nelissen L, Lemstra PJ, Liska J, Bailly C. Polymer 2001;42:2803–13.
[26] Yamanaka K, Inoue T. Polymer 1989;30:662–7.
[27] Lee H, Neville K. Handbook of epoxy resins. New York: McGraw-Hill; 1967. Chapter 5.
[28] Hale W, Keskkula H, Paul DR. Polymer 1999;40:365–77.
[29] Dante MF, Parry LP. US Patent 3,477,990; 1969.
[30] Lopez JA. US Patent, 4,320,222; 1982.
[31] Shih PS. US Patent, 3,836,485; 1974.
[32] Lee PC, Kuo WF, Chang FC. Polymer 1994;35:5641–50.
[33] Chang DY, Chang FC. J Appl Polym Sci 1995;56:1015–28.
[34] Maa CT, Chang FC. J Appl Polym Sci 1993;49:913–24.
[35] Chen SH, Chang FC. J Appl Polym Sci 1994;51:955–65.
[36] Liu WB, Kuo WF, Chiang CJ, Chang FC. Eur Polym J 1996;32:91–9.
[37] Tsai CH, Chang FC. J Appl Polym Sci 1996;61:321–32.
[38] Macosko CW. Macromol Symp 2000;149:171–84.
[39] Macosko CW, Guégan P, Khandpur AK, Nakayama A, Marechal P, Inoue T. Macromolecules 1996;29:5590–8.
[40] Scott CE, Macosko CW. Polymer 1995;36:461–70.
[41] Lee H, Neville K. Handbook of epoxy resins. New York: McGraw-Hill; 1967, 5–6.
[42] Saunders JH, Frisch KC. Polyurethans: chemistry and technology. New York: Interscience; 1962.
[43] Chen TH, Su AC. Polymer 1993;34:4826–31.
[44] Nakayama A, Guegan P, Hirao A, Inoue T, Macosko CW. ACS Polym Prepr 1993;34:840.
[45] Ibuki J, Charoensirisomboon P, Chiba T, Ougizawa T, Inoue T, Weber M, Koch E. Polymer 1999;40:647–53.
[46] Charoensirisomboon P, Inoue T, Weber M. Polymer 2000;41:6907–12.